J. Phys. B: At. Mol. Opt. Phys. **44** (2011) 145701 (9pp) doi:10.1088/0953-4075/44/14/145701

Early time properties of ultracold neutral plasmas

K Niffenegger, K A Gilmore and F Robicheaux

Department of Physics, Auburn University, AL 36849-5311, USA

E-mail: robicfj@auburn.edu

Received 28 April 2011, in final form 30 May 2011
Published 29 June 2011
Online at stacks.iop.org/JPhysB/44/145701

Abstract

We present simulations of some of the early time properties of ultracold neutral plasmas. We focus on three aspects of this system. First, we study the earliest electron dynamics when the initial temperature of the electrons would place them in the strongly coupled regime. We focus on times out to ∼10 plasma periods of the electron but also present results out to ∼85 plasma periods. In particular, we study how the formation of Rydberg atoms leads to heating and how the mass of the ion could enter the dynamics. Second, we study how the ions behave when the electrons are at high temperatures by comparing simulations that treat the electrons as a fluid and simulations that simultaneously include the electrons and ions. For light ions, the electron–ion scattering transfers substantial energy from the electrons to the ions. Finally, we study the ion motion at early times and at low temperatures where the electron evolution and ion motion could be at comparable time scales. This allows a test of electron–ion scattering when the electron plasma is nearly strongly coupled and we find that the recent values for the electron–ion scattering rate underestimate the ion heating in our calculations.

1. Introduction

Ultracold neutral plasmas can be used to test aspects of plasma and atomic physics for parameters where some of the simple concepts at the heart of plasma and atomic physics may no longer apply [1]. One of the appealing aspects of this system is that the plasma is initiated from cold atomic or molecular gases using laser ionization or excitation of the atoms or molecules. Thus, many aspects of the system are relatively easy to control. For example, the density can be controlled through the density of the gas and the laser power that ionizes or excites the atoms. Another example, the initial temperature of the electrons can be controlled by changing the wavelength of the laser.

For plasmas, one of the more interesting parameters that characterizes the plasma behaviour is the Coulomb coupling parameter

$$\Gamma = \frac{e^2/(4\pi\varepsilon_0 a_{\rm ws})}{k_{\rm B}T}, \tag{1}$$

where $a_{\rm ws}$ is the Wigner–Seitz radius,

$$a_{\rm ws} = \left(\frac{3}{4\pi n}\right)^{1/3}, \tag{2}$$

e is the electron charge, $k_{\rm B}$ is Boltzmann's constant, n is the number density, and T is the temperature. If Γ is larger than ∼1, then the components of the plasma start displaying correlated motion and that component of the plasma is considered to be strongly coupled. If Γ is less than ∼1, then the plasma is weakly coupled. In the weakly coupled limit, standard plasma concepts (e.g. Debye screening, electron–ion scattering, etc) and standard atomic concepts (e.g. three-body recombination) are expected to be good approximations.

One of the early experiments on ultracold neutral plasmas probed how the expansion of the plasma varied with the initial energy of the electron relative to the vacuum threshold [2]. Since the electrons quickly thermalize, the electron temperature was expected to be $k_{\rm B}T_e \simeq (2/3)E$, where E is the initial electron energy relative to threshold. They found the plasma expanded more quickly than expected at low initial E. In a later paper [3], a substantial fraction of Rydberg atoms were shown to form in the plasma although the time dependence of the atomic properties was non-intuitive. Several theory papers [4–9] showed that these results could be explained by the interplay of standard atomic and plasma physics and were not due to effects from a strongly coupled plasma.

In recent years, there have been a number of studies of ultracold neutral plasmas at early times (less than 1 μs). These studies have demonstrated an oscillation in the average kinetic

energy of the ions [10–14] due to their motion away from their random initial placement at $t = 0$. Again, these results seem to be understandable using Debye screened interaction potentials between the ions.

Recently, references [15, 16] reported results in a molecular beam that seems to contradict the expectations from standard plasma and atomic physics. In this experiment [16], the expansion of the plasma seems to be too slow for the expected electron temperature at their density. The density of their plasma is $\sim 10^3\times$ greater than previous ultracold neutral plasmas and they have molecular ions instead of atomic ions. It seems that neither of these changes should lead to slower plasma expansion so these results remain unexplained [17].

In this paper, we address three issues. First, we revisit how a plasma with the electrons launched at the vacuum threshold energy behaves at early times. Second, we investigate how the ions behave and whether we can model their motion using Debye screened potentials plus a Langevin heating to model electron–ion scattering when the electrons are very weakly coupled (i.e. $\Gamma_e < 0.1$). Third, we investigate the ion motion at early to intermediate times as a possible test of current electron–ion collision rates in a plasma.

2. Computational method

We simulated the motion of the ions and electrons using classical equations of motion. We used an adaptive step-size fourth-order Runge–Kutta algorithm [18] to move the particles forward by one time step. This method is not symplectic so care must be taken to ensure that the results are not affected by unphysical, numerical drag. The accuracy of the method was checked by making sure the energy drift per particle was less than 0.01 K for every run; this upper limit of the error was never reached and the typical energy drift was approximately 1 mK which is less than 0.05% of the average kinetic energy of an electron. We also performed runs at differing levels of accuracy and made sure that the properties of interest were converged.

As is typical, we did not use a pure Coulomb force for the particles all of the way to zero separation. We derived the force from a spherically symmetric potential between particles i and j that had the form

$$PE_{ij} = \frac{q_i q_j}{4\pi\varepsilon_0\sqrt{r_{ij}^2 + (Ca_{\rm ws})^2}}, \tag{3}$$

where q_i is the charge of particle i, r_{ij} is the separation of particles i and j, $a_{\rm ws} = [3/(4\pi n)]^{1/3}$ is the Wigner–Seitz radius which is found from the number density n, and C is a constant substantially less than 1. We performed calculations for several values of C from 0.01 to 0.05 to determine the effect that the soft core had on the dynamics. The role that the constant C plays in the calculation is discussed in the results of the different simulations below. We emphasize that this form of the potential is a numerical device for speeding up the calculation while keeping the physical result the same. In other contexts, quantum mechanical effects lead to a change from a pure Coulomb potential but these are typically only important in plasmas much denser than those considered here; reference [19] gives this type of potential within the context of ultracold neutral plasmas. To see that quantum effects are not important for our parameters, we can compare the de Broglie wave length for an electron at 5 K ($\lambda \simeq 60$ nm) to the Wigner–Seitz radius at a density of 10^9 cm^{-3} ($a_{\rm ws} \simeq 6200$ nm), which means there are approximately 10^6 quantum states available for each particle; another comparison is the Fermi energy at 10^9 cm^{-3} ($E_F \simeq 4.2 \times 10^{-5}$ K) compared to the typical electron kinetic energy of a few K. A final point of comparison is the distance of closest approach of two electrons at 5 K ($r = e^2/(4\pi\varepsilon_0 k_{\rm B} T_e) \simeq 3300$ nm) compared to the de Broglie wavelength ($\lambda \simeq 60$ nm). All of these comparisons show that the Pauli exclusion principle and other quantum effects will have negligibly small effects on our calculations.

In our simulations, we calculate the behaviour for a finite number of particles so the treatment of the boundary could be important. As is typical, we used a wrap boundary condition on a cube when computing the forces. During each time step, we checked whether the x, y or z position was less than 0; if yes, we added the length of the cube, L, to that component of the position keeping the velocity unchanged. If the x, y or z position was greater than L, we subtracted L from that component. When we computed the force or potential energy between two particles, we would use $x_i - x_j$ if $-L/2 \leqslant (x_i - x_j) \leqslant L/2$ but would use $x_i - x_j + L$ if it was less than $-L/2$ and $x_i - x_j - L$ if it was greater than $L/2$. Similar definitions applied to the y- and z-components. As the number of particles in the simulation increases for a given density, the size of the cube increases and the effect of the edges becomes less. We checked convergence with respect to the cube size by comparing the results from different size runs and by artificially cutting off the force at a separation less than $L/2$. For us it was a surprise that the most difficult calculation to converge with respect to cube size was the ion motion, in particular, the average ion kinetic energy as a function of time. These results will be described below.

Ultracold plasmas are made by photoionizing a cold atomic gas. To mimic this behaviour, we start our plasma by placing 'atoms' randomly within the cube. We have treated the atoms as having zero velocity or as having a thermal velocity distribution given by an ultralow temperature typical for cooled atomic gases (e.g. 100 μK); for the densities we investigated, we found that the disorder-induced heating of the ions tended to be a much larger effect than the initial velocity distribution and the difference between simulations with initial 0 K or with 100 μK was negligible. For the calculations that only treated the ions (electrons included as a Debye screening effect), this is the only information needed to start the simulation. For the calculation that explicitly included ions and electrons, the launch dynamics is somewhat more complicated. To correctly account for the photoionization, the electron is started near the ion (typically within 20 Bohr radii) with a velocity in a random radial direction from the ion, $\vec{v}_e = v\hat{r}$. To conserve momentum, the ion is given the opposite momentum of the electron, $\vec{v}_i = -v\hat{r}m_e/m_i$, where m_e/m_i is the ratio of electron to ion masses. The magnitude

of the velocity is chosen so that the energy of the atom

$$E = \tfrac{1}{2}\left(m_e v_e^2 + m_i v_i^2\right) + PE(r_{ij}) = \frac{m_e + m_i}{m_i}\frac{m_e v^2}{2} + PE(r_{ij}) \quad (4)$$

equals the energy relative to the vacuum threshold of the 'atom' after the photon is absorbed.

We introduce a difference from experiment by using this prescription for starting the simulation. In a real experiment, there is an energy width from the bandwidth of the laser. We tested this in our simulations and found that the bandwidth was not a large effect unless the energy width was substantially larger than the average energy and the average kinetic energy from disorder-induced heating. Also in a real experiment, the laser has a duration which means the photons are not all absorbed at one time. To include this last effect appropriately, the electron–ion pairs should be launched with a distribution of times corresponding to the laser duration. This could be an important effect in some experiments because at the higher densities and longer laser pulse lengths the duration could be many plasma periods. Unfortunately, the variation between different types of experiments precludes a systematic study of this effect at this time.

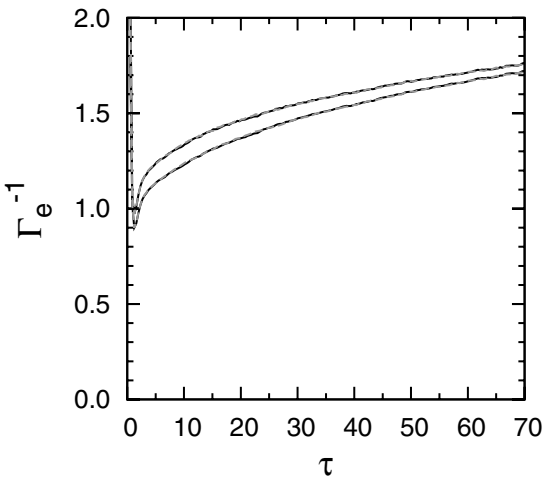

Figure 1. Four calculations of the scaled electron temperature, $\Gamma_e^{-1} = k_B T_e/[e^2/(4\pi\varepsilon_0 a_{ws})]$, are shown as a function of the scaled time $\tau = \omega_{pe} t$. The plasma parameters are in the text. The solid black lines are for a simulation with 100 ions and 100 electrons; the upper curve is when the electrons closer to an ion than $0.1a_{ws}$ were excluded from the calculation of the temperature and for the lower curve the exclusion region was $0.2a_{ws}$. The dashed grey lines are for a simulation with 200 ions and 200 electrons; the upper and lower curves have the same meaning as the 100-atom simulation. The difference between the 100-atom and 200-atom simulations is hardly visible on this graph.

3. Low temperature electrons

Reference [7] gave the results of calculations for the free electron temperature as a function of time when the electrons start at 0 K. The main interest for us is at very early times because at later times the temperature rises [5] to the point where the coupling constant for the electrons $\Gamma_e = e^2/(4\pi\varepsilon_0 a_{ws} k_B T_e) \sim 1/5$ with k_B being Boltzman's constant, T_e the free electrons' temperature and a_{ws} the Wigner–Seitz radius. We were motivated to revisit this calculation because current computational resources allow us to lift some of the approximations used although we do not expect large differences from the results in [7]. In particular, there were three aspects of the calculation that we revisited: (1) the starting condition of the electrons was not that of a photoionized gas (they started the randomly distributed electrons independent of the ions), (2) the soft core size was $C = 1/31$ (smaller values can be used) and (3) the ion mass $m_i = 100 m_e$ (larger values for the ion mass can be used).

The main results we wish to make a comparison with is their figure 1 which shows $1/\Gamma_e = k_B T_e/[e^2/(4\pi\varepsilon_0 a_{ws}]$ starting from 0 and rising to ∼1 on a time scale of $\sim 1/\omega_{pe}$, where $\omega_{pe} = \sqrt{ne^2/(\varepsilon_0 m_e)}$ is the electron plasma frequency; the temperature then approximately linearly increases with time so that $1/\Gamma_e \simeq 1.4$ at the time $70/\omega_{pe}$.

One of the difficulties of making a direct comparision with this calculation is deciding what is meant by the electron temperature. Reference [7] took all electrons that were not deeply bound to an ion and found their velocity distribution; they fitted this distribution to a Maxwell–Boltzman distribution to obtain the temperature. We obtained the temperature by using the equipartition theorem for electrons that were further than a specified distance from every ion; the distance we chose was either $a_{ws}/10$ or $a_{ws}/5$ (comparing the two calculations gives an estimate of the uncertainty of the temperature as discussed below). We compared this temperature to a fit to the Maxwell–Boltzman distribution at different times and found that the agreement was more accurate than errors from other aspects of the calculation. Thus, all of the results we present use the definition of temperature to be 2/3 of the average kinetic energy for electrons outside of a specified region near any ion.

In [7], 4096 electrons and 4096 ions were used. We were surprised that the free electron temperature could be converged with as few as 100 electrons and 100 ions. We repeated the simulation for approximately 1000 runs with different random initial conditions and averaged the results together to give the values that we plot. Figure 1 shows four calculations of the scaled electron temperature where the ion mass was taken to be 40 times the mass of the proton, the soft core was taken to be $C = 0.03$, and the density was taken to be 10^9 cm^{-3}. The electrons are launched from the ion so that the electron plus ion has 0 energy if it was an isolated atom. For this density, $a_{ws} = 6.20$ μm, the plasma frequency $\omega_{pe} = 1.78 \times 10^9$ s^{-1} and the scaled temperature $e^2/(4\pi\varepsilon_0 a_{ws} k_B) = 2.69$ K.

The four different scaled temperatures plotted in figure 1 result from two different simulations; one simulation had 100 electrons and 100 ions and the other simulation had 200 electrons and 200 ions. For each simulation we calculated the electron temperature in two different ways: in the first, temperature was only calculated from electrons that were further than $0.1a_{ws}$ from every ion and in the second, was only calculated from electrons that were further than $0.2a_{ws}$ from every ion. It is necessary to exclude some regions around

the ions because the tightly bound electrons will have high kinetic energy even though they have negative total energy. This exclusion is similar to the prescription in [7] although there is insufficient information for an exact comparison.

There are two important features to note. The first is that the 100 and 200 electron runs give nearly identical answers when the temperature is computed in the same way. This shows that for the free electron temperature we can obtain accurate results by averaging calculations with as few as 100 electrons and ions. To make sure that the electron temperature was converged, we also performed this calculation with 400 electrons and ions and with 800 electrons and ions; the runs with more electrons and ions agreed perfectly with those presented in figure 1. The second feature to note is that there is a difference in temperature when using the different regions of exclusion. The difference is largest for $\omega_{pe}t \sim 15$, where the ratio of the temperatures is ∼1.08 and the difference decreases with time becoming about 2% at $\omega_{pe}t \sim 70$.

The behaviour of the temperature dependence when only counting electrons outside of $0.1a_{\rm ws}$, compared to when we only count electrons outside of $0.2a_{\rm ws}$, is due to understandable physics principles. When the electrons are in thermal equilibrium, the average kinetic energy in any region of space should be $(3/2)k_{\rm B}T$. This system does not start in thermal equilibrium and evolves toward equilibrium with time. The region of space near the ions is the last to reach thermal equilibrium. Since the calculation, where we only count electrons outside of $0.2a_{\rm ws}$, excludes more of the problematic region, we expect this to be a more accurate estimate of the free electron temperature. The calculation, where we only exclude the region outside of $0.1a_{\rm ws}$, overestimates the temperature because there are not enough electrons from the deeply bound states that enter the region $0.1a_{\rm ws} < r < 0.2a_{\rm ws}$ with low velocity. In all that follows, the temperatures of the electrons are presented for those outside of $0.2a_{\rm ws}$.

The general trend of the temperature is nicely explained in [7]. At the earliest times, the disorder-induced heating of the electrons occurs over a time range of the order of one plasma period. At later times, the free electron temperature increases due to the formation of Rydberg atoms. The electron in an atom is at negative energy. To conserve energy, the free electron temperature should increase. We find that the number of electrons in the excluded region increases with time which is the result of the formation of atoms. In [7], the electron temperature rises from 0 to 1 because they start the electrons randomly placed with zero velocity; in our calculation, the electron temperature rapidly decreases to 1 because we launch the electrons from near the nucleus where they must have high velocity to escape.

In figure 2, we show the effect of the ion mass on the free electron temperature. In all calculations, the density was 10^9 cm^{-3}, the soft core parameter $C = 0.03$, and the simulations used 100 ions and electrons. The temperature was found from only the electrons outside of $0.2a_{\rm ws}$ from every ion. The electron temperature is shown for the cases where the ion mass is $m_i = 100m_e$ which is the value used in [7], the proton mass, 40 times the proton mass, and 400 times the proton mass. Our calculation of the temperature for $m_i = 100m_e$ is in decent,

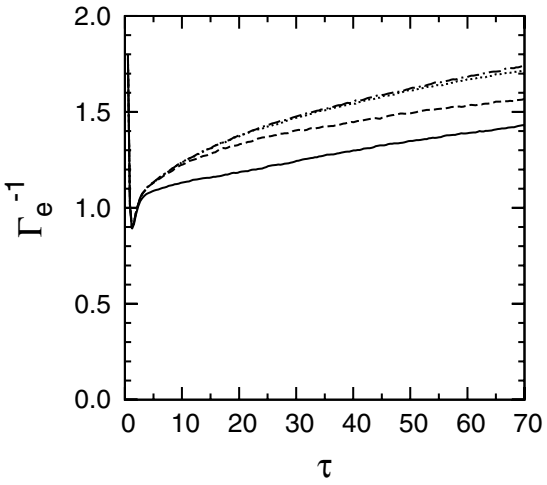

Figure 2. Same as figure 1, but all calculations are for 100 ions and electrons. We vary the mass of the ion for this plot. The solid line is for a mass of $100m_e$, the dashed line is for a mass of $1m_p$, the dotted line is for a mass of $40m_p$ and the dash-dotted line is for a mass of $400m_p$, where m_e and m_p are the masses of the electron and proton, respectively.

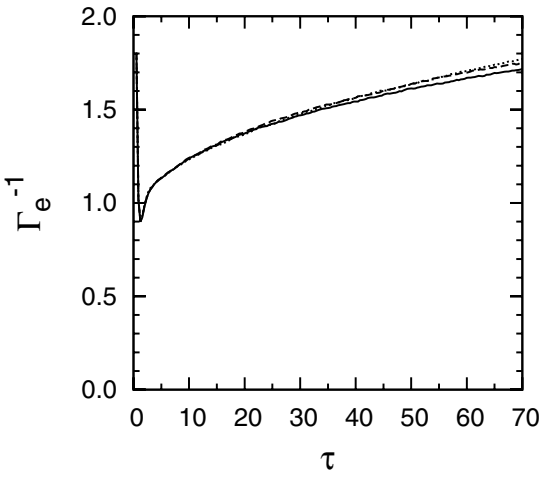

Figure 3. Same as figure 2, but all calculations are for the mass of the ion being $40m_p$. We vary the soft core parameter for this plot. The solid line is for $C = 0.03$, the dashed line is for $C = 0.02$ and the dotted line is for $C = 0.01$.

but not perfect, agreement with [7]; their scaled temperature was 1.40 at $t\omega_{pe} = 70$ whereas our value is 1.44; this 3% difference could be due to the slight difference in how we compute the temperature or could be due to how we start the electrons at $t = 0$.

There is perhaps a surprising difference between the calculations with different masses. The main physical effect is the heating of the ions through electron–ion collisions. As will be seen below, there is a substantial amount of energy transfer from the electrons to the ions and the energy transfer is more effective when the ion mass is smaller. Thus, for the case with $m_i = 100m_e$, the electrons transfer much more energy to the ions than when the ion has one proton mass, etc. Typical experiments are performed with ions that have tens of proton mass. Thus, the scaled temperature in experiments will be at ∼1.7 at $t\omega_{pe} = 70$.

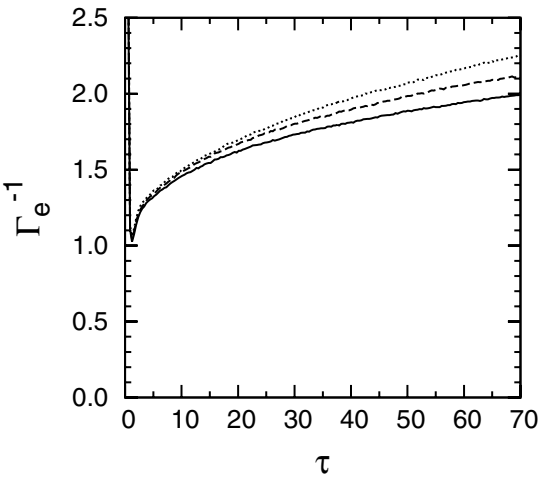

Figure 4. Same as figure 3, but we compute the temperature from the average kinetic energy of all electrons. We vary the soft core parameter for this plot. The solid line is for $C = 0.03$, the dashed line is for $C = 0.02$ and the dotted line is for $C = 0.01$.

In figure 3, we show the effect of the soft core parameter C on the free electron temperature. The three curves are for $C = 0.03, 0.02$ and 0.01. The trend is for the smaller value of C to correspond to a higher free electron temperature. This figure shows that the free electron temperature does not strongly depend on the soft core parameter at these low values; there is only a 3% difference between the $C = 0.03$ and 0.01 results. An interesting feature is what little difference exists between the calculations becomes apparent only at later times as the number of Rydberg atoms formed in the plasma increases.

However, this does not mean that the dynamics is unaffected by the soft core parameter. As noted in [7], the soft core parameter affects the population of bound atoms and it affects the lowest possible energy for an electron: for $C = 0.03$, the lowest possible energy is $\simeq 33.3e^2/(4\pi\varepsilon_0 a_{\rm ws})$ while for $C = 0.01$, the lowest possible energy is $\simeq 100e^2/(4\pi\varepsilon_0 a_{\rm ws})$. Figure 4 shows the scaled temperature defined from 2/3 of the average kinetic energy of all of the electrons for the soft core parameters of figure 3. In this figure, there is approximately a 12% difference between the $C = 0.03$ and 0.01 results. Perhaps it is more disturbing that there is not a clear convergence as C decreases. We found that the calculated fraction of free electrons differed by less than 1% for the three different soft core parameters. At the final time in this figure, the fraction of free electrons is approximately 0.84; the excluded volume times the density gives 0.992 free electrons just due to random probability of electrons being in that volume. This suggests that approximately 15% of the electrons have become reattached to an atom at the latest time. The calculations with smaller C have higher average kinetic energy because there are slightly more deeply bound electrons when C is smaller, and these electrons have an average kinetic energy approximately equal to their binding energy.

Taking into account the effects of larger ion mass and smaller soft core parameter C, we suggest that the experimental electron temperature is approximately 25% hotter than the result from [7], figure 1. The final time $t\omega_{pe} = 70$ corresponds to ∼11 plasma periods; at this time, we have the electron Coulomb coupling parameter $\Gamma_e \simeq 0.56$ compared to 0.71 from [7] figure 1. The results of figures 1–3 can be scaled to apply to any cold plasma where quantum mechanical effects are not important. The typical effects that would not allow scaling could include populating quantized energy levels of the atom, photon emission from bound states, dielectronic recombination, dissociative recombination, scattering of electrons or ions off of background neutrals, etc.

We have also performed calculations to final times approximately eight times longer than the results presented in this section. These results are given below in section 5.

4. Ion motion

There have been several calculations that have modelled the ion motion when the electrons are at high temperature using a screened Coulomb potential. We took the ion–ion potential energy to have the form

$$PE = \frac{e^2}{4\pi\varepsilon_0}\frac{{\rm e}^{-r_{ij}/\lambda_{\rm De}}}{r_{ij}} \tag{5}$$

where $\lambda_{\rm De} = \sqrt{\varepsilon_0 k_{\rm B} T_e/(ne^2)}$ is the Debye length and r_{ij} is the separation of the ions i and j. If the ions start essentially at rest in random positions, their average kinetic energy oscillates [10–12] due to the initial fluctuation in the density of the ions. We have performed calculations for somewhat longer times in order to understand the role that electron scattering plays in the ion motion. We chose the ion to have the mass of one proton in order for the ion plasma period and the electron scattering time scale to be somewhat comparable.

To first understand how the properties depend on the number of particles, we performed a calculation using the screened potentials for an electron temperature of 100 K and a density of 10^9 cm^{-3}. For these parameters, the Debye length is 21.8 μm. The ion temperature is defined as 2/3 of the average kinetic energy. In figure 5, we show the average ion temperature versus time for the first few oscillations of the ions. Our results are for 100 ions (average of 960 runs), 400 ions (average of 240 runs), 1500 ions (average of 64 runs) and 6000 ions (average of 16 runs). The ion oscillation in an ultracold neutral plasma was studied theoretically in [12] and experimentally in [10, 11]. For us, the interesting aspect of figure 5 is the extremely slow convergence with respect to the number of particles. The cube length in the simulation is $L = (N/n)^{1/3}$, where N is the number of particles in the simulation. For $N = 100$, $L = 46.4$ μm which is slightly more than twice the Debye length so it is understandable that the 100 ion run is problematic. However, $N = 400$ gives $L = 73.7$ μm, $N = 1500$ gives $L = 114$ μm and $N = 6000$ gives $L = 182$ μm. Even though the $N = 1500$ case gives a cube length that is more than five times the Debye length, the results are not quite converged. The reason is that the range of wavelengths of the density fluctuations that can be supported in different cube sizes determines the convergence. The smaller cubes can support only shorter wavelength waves which are at higher frequency (i.e. smaller period). If we had simulated

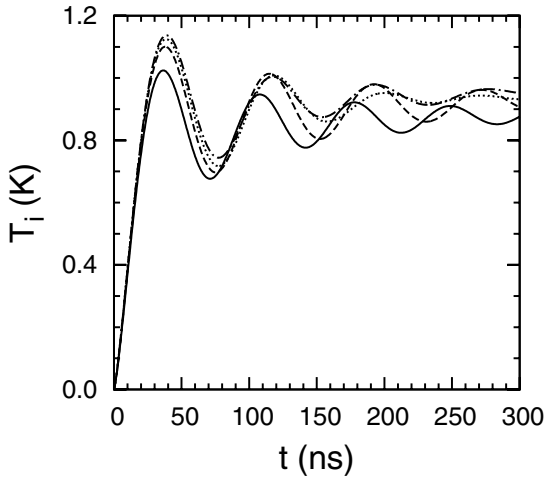

Figure 5. The ion temperature (defined as 2/3 the average ion kinetic energy) versus time after the plasma is started for a calculation using Debye screened potentials for the ions. The electron temperature is 100 K, the density is 10^9 cm^{-3}, and the ion mass is m_p. The solid line is for a 100-ion calculation, the dashed line is for a 400-ion calculation, the dotted line is for a 1500-ion calculation and the dash-dotted line is for a 6000-ion calculation.

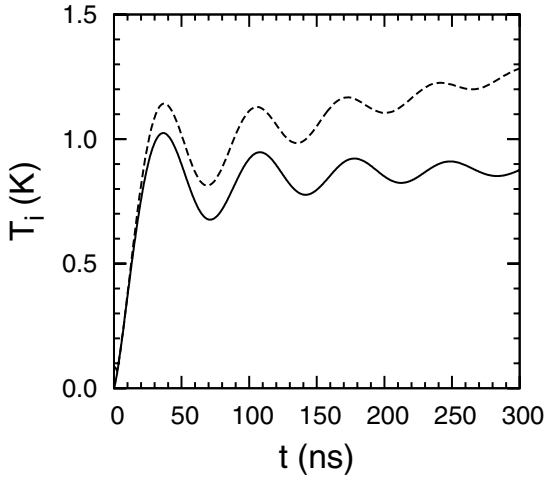

Figure 6. Same as figure 5 for 200 ions. The solid line is from an ion-only calculation that uses the Debye screened Coulomb interaction for the ion–ion force and the dashed line is from a full simulation using 200 ions and 200 electrons. The increasing temperature in the full simulation is from electron–ion scattering which transfers energy from the 100 K electrons to the ions.

a much lower temperature (e.g. 25 K), the ion motion would have converged with fewer particles.

We do not have the computer resources needed for a full electron and ion run with 6000 particles so we will compare the full electron–ion run with 200 electrons and 200 ions to the screened ion run with 200 ions. The ion temperature from these two types of calculations is compared in figure 6. The two results give a similar period for the ion oscillation but the full calculation shows an increasing temperature as a function of time. The electron temperature shows a decrease of approximately 0.3 K between 20 and 300 ns while the difference between the ion temperature in the full calculation and the screened ion calculation is approximately 0.4 K at 300 ns. This comparison is similar in spirit to that performed in [19], where Murillo compared the evolution of the ion kinetic energy using a Yukawa model and full electron–ion dynamics; the main difference is that [19] used a larger ion mass so the electron–ion scattering was not so important.

Reference [20] gives an expression for the heating rate of ions due to collisions with electrons as

$$\frac{\mathrm{d}T_i}{\mathrm{d}t} = -\nu_{ie}(T_i - T_e), \tag{6}$$

where T_i and T_e are the ion and electron temperatures, respectively, and

$$\nu_{ie} = \frac{ne^4\sqrt{2\pi m_e m_i}}{6\pi^2\varepsilon_0^2(m_i k_\mathrm{B} T_e)^{3/2}} \ln(1 + 0.7\lambda_\mathrm{De}/r_L), \tag{7}$$

where $r_L = e^2/(4\pi\varepsilon_0 k_\mathrm{B} T_e)$ is the distance of the closest approach and the term in the logarithm comes from a fit to their molecular dynamics data shown in figure 3 of [20]. In their molecular dynamics simulation, the sign of the electrons' charge is reversed to prevent recombination at low temperatures; they argue that reversing the sign of the electron should not affect the results since the exact scattering cross section depends on the square of the charge. Evaluating the collision rate for an electron temperature of 100 K, density of 10^9 cm^{-3} and m_i equalling the proton mass gives $\nu_{ie} = 1.8 \times 10^4$ s^{-1}. Using $T_e - T_i = 99$ K, we find that the change in ion temperature due to scattering is 0.53 K after 300 ns. This is not too far from the result seen in figure 6.

We attempted to include the electron scattering in our screened ion simulation by using a Langevin heating scheme in an attempt to quantitatively reproduce the full ion–electron simulation. This idea uses the fluctuation dissipation theorem and is similar in spirit to the treatment in [23] (but they only include the fluctuation because they have ion cooling from an external laser). During a time step of duration δt, every component of the velocity is decreased by the factor $\exp(-\nu_{ie}\delta t/2)$ and a random velocity is added to it from a Gaussian distribution proportional to $\exp(-v^2/\Delta v^2)$ with

$$\Delta v^2 = \frac{2k_\mathrm{B} T_e}{m_i}[1 - \exp(-\nu_{ie}\delta t)], \tag{8}$$

where the fluctuations and dissipation are chosen to lead to the equipartition theorem at long times. Because there is some transfer of energy from the electrons to the ions due to the collisions, we should have a time-dependent electron temperature which will lead to a time-dependent Debye screening length and to a time-dependent scattering rate. For times less than 300 ns, we found that the electron temperature did not change by more than 2% for T_e from 10 to 100 K so it was not necessary to take this effect into account. However, we found that the electron temperature was noticeably different from the input temperature; the 100 K simulation actually gave 100.6 K electrons and the 10 K simulation actually gave 11.6 K electrons. When we included the electron scattering in the Debye screened code for the ion motion, we found good agreement with the heating rate using equation (7) for 100 K but there was increasing disagreement at low temperatures.

In figure 7, we show the comparison between the full electron–ion run, screened ions without electron heating,

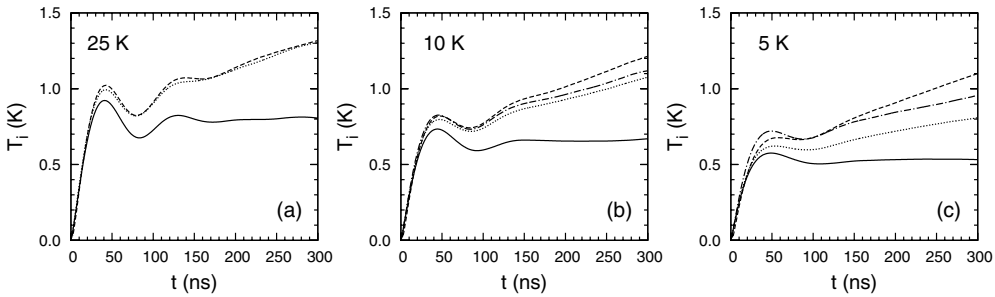

Figure 7. Same as figure 6 for initial electron temperatures of 25, 10 and 5 K. The solid line is from an ion-only calculation that uses the Debye screened Coulomb interaction for the ion–ion force, the dashed line is from a full simulation using ions and electrons ($C = 0.02$) and the dotted line includes a Langevin heating in the ion-only calculation. The dash-dotted line on the 10 and 5 K plots are Langevin heating calculations at the average electron temperatures of 11.6 and 7.5 K, respectively. We increased the number of ions and electrons until convergence was achieved. The 25 K run used 400 ions and electrons, and both the 5 and 10 K run used 200 ions and electrons.

and screened ions with electron heating. We used lower temperatures where interesting behaviour is expected and where it is easier to converge the full electron–ion calculation with respect to the number of particles because the electron Debye length is smaller. Figure 7(a) shows the $T_e = 25$ K results; for this calculation, the length of the cube is 73.7 μm and the Debye length is 10.9 μm. The full electron–ion run clearly shows the effect of heating. The screened ion calculation without heating clearly shows the effect of the ion oscillation with approximately the same period as the full calculation, but the temperature plateaus since there is a conserved energy. Including the heating gives very good agreement although the period is slightly shifted. Figure 7(b) shows the $T_e = 10$ K results. Including the electron heating gives better agreement although the amount of heating underestimates the actual heating rate by a factor of $\sim$1.38 (actual increase in temperature $\sim$0.55 K but the screened ion calculation with heating has an increase in temperature of $\sim$0.40 K). One possible cause for the discrepancy is that the actual electron temperature in the full calculation is approximately 11.6 K from disorder-induced heating of the electrons and approximately 3% recombined atoms; this temperature corresponds to $\Gamma_e \simeq 0.23$. The result of using this electron temperature is shown as a dot-dashed line; while using the actual electron temperature improves the agreement, the heating is underestimated by a factor of $\sim 0.55/0.45 = 1.22$.

Figure 7(c) shows the $T_e = 5$ K results. In the full ion–electron calculation, the electron temperature starts at $\sim$7 K after 1 ns and rises to $\sim$7.9 K at 300 ns. Approximately 8% of the ions have captured an electron and become atoms by 300 ns. None of the screened ion calculations match the full calculation very well. The screened ion with Langevin heating for 5 K electrons reproduces the initial slope of the ion temperature (good agreement to $\sim$30 ns) but underestimates the heating rate by a factor of $\sim$2. The screened ion with Langevin heating for 7.5 K electrons does not reproduce the initial slope and overshoots the temperature at early times and is too cold at later times; this temperature corresponds to $\Gamma_e \simeq 0.35$. The heating rate from 150 to 300 ns is too small by a factor of $\sim$1.7. The results in figures 7(b) and (c) indicate that the scattering formula in [20] may not be accurate for $\Gamma_e > \sim 0.2$.

There have been other recent studies of electron–ion scattering. The authors of [21] performed calculations for densities of 10^{20}–10^{24} cm^{-3} and found that the parameterization in [22] worked well; in these studies, the electrons and ions had opposite sign charges unlike reference [20] and, therefore, might more accurately apply to our results. However, they are at densities a factor of 10^{11}–10^{15} higher than ours so that quantum effects are more important and might affect how they weight the fitting of the scattering logarithm. Their expression for the logarithm is

$$\mathcal{L} = \frac{1}{2}\ln\left(1 + \frac{\lambda_{\rm De}^2 + a_{\rm ws}^2}{r_L^2}\right), \tag{9}$$

where we have dropped the thermal de Broglie wavelength from their expression because it had negligible effect on the results. The logarithms in equation (7) and equation (9) look different, but they have the high-temperature limits of $\ln(\lambda_{\rm De}/r_L) + \ln(0.7)$ and $\ln(\lambda_{\rm De}/r_L)$, respectively. At 25 K, the result in equation (9) is 16% higher than the result used in figure 7(a), which means it will give a scattering rate that is approximately 16% too high. At 11.6 K, the result in equation (9) is 25% higher than the result used in figure 7(b), which means it will give an almost perfect scattering rate. At 7.5 K, the result in equation (9) is 31% higher than the result used in figure 7(c), which means it will give a scattering rate that is approximately 25% too low compared to the full ion–electron calculation. Thus, neither of the expressions for electron–ion scattering ([20] or [22]) give perfect input to our Langevin modelling of the ion heating. It could be that the defect in [20] uses the same charge for the electron and ion and the defect in [22] is the extrapolation from high density. However, we cannot rule out that the defect is in the simple Langevin scattering model of the ion heating.

The results of figures 7(b) and (c) indicate that the heating of ions due to electron scattering may be underestimating the heating rate for Coulomb coupling parameters that are relevant for ultracold plasmas at early times and at late times when the plasma is expanding. If ion heating due to electron scattering is underestimated by the current formulas, the interesting proposals [24, 25] about strong coupling in ions could be affected.

For the calculations of figure 7, we tested how the soft core parameter C affected the long-time behaviour of the ion

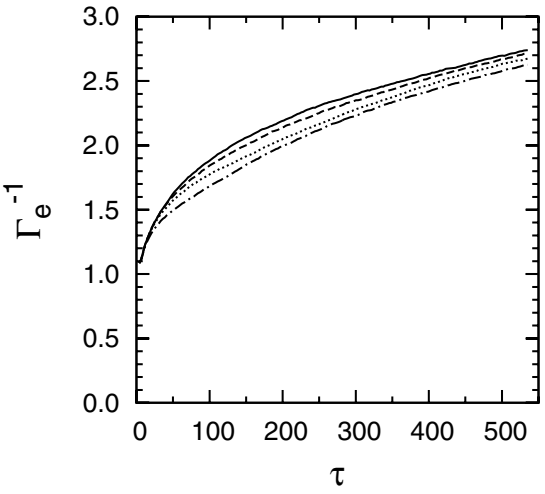

Figure 8. Four calculations of the scaled electron temperature, $\Gamma_e^{-1} = k_B T_e/[e^2/(4\pi\varepsilon_0 a_{ws})]$, are shown as a function of the scaled time $\tau = \omega_{pe}t$ when the electrons are launched at zero energy relative to the vacuum threshold. The simulation is for 100 ions and 100 electrons. The screening parameter $C = 0.02$ was used and the initial electron density was 10^9 cm^{-3}. The solid line is for an ion mass of $40m_p$, the dashed line is for an ion mass of $16m_p$, the dotted line is for an ion mass of $4m_p$, and the dash-dotted line is for an ion mass of $1m_p$.

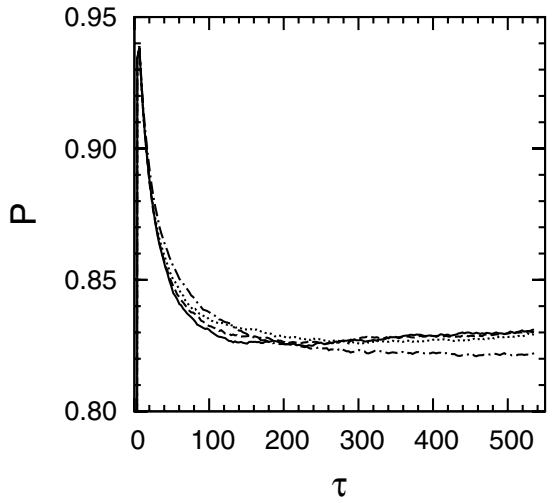

Figure 9. The same physical situation and line types of figure 8 but plotting the fraction of free electrons, P, as a function of the scaled time. An electron is counted as free if it is more than $0.2a_{ws}$ from every ion.

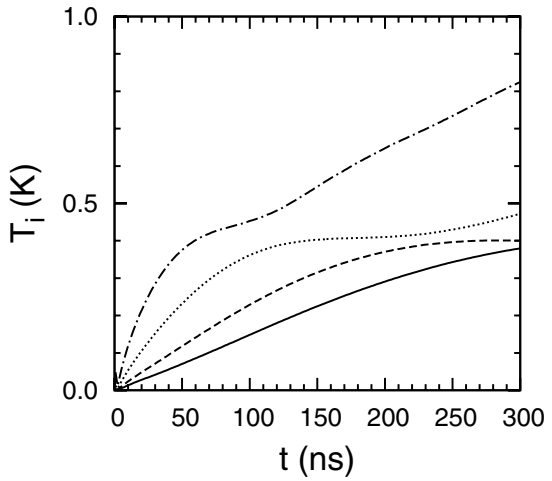

Figure 10. The same physical situation and line types of figure 8 but plotting the ion temperature (defined as 2/3 of the average ion kinetic energy) as a function of time. The time range shown is the same as in figures 8 and 9.

temperature. From figure 3, we showed that most of the convergence occurred when going from $C = 0.03$ to 0.02. All of the results in figure 7 used $C = 0.02$. We found that changing C from 0.03 to 0.02 changed the electron temperature for the final time of figure 7 by approximately 1% and approximately 5% for the 10 and 5 K calculations, respectively. The change for the ion temperature was approximately 2% for both the 10 and 5 K calculations. Thus, these calculations are converged with respect to C.

5. $T = 0$, longer times

One of the interesting aspects of the ultracold plasmas is the question of how this system behaves when the electrons are launched exactly at the vacuum threshold. In section 3, we gave the electron motion for times out to $\omega_{pe}t_{fin} \simeq 70$ which corresponds to 40 ns. The calculations in this section extend to 300 ns which is ($\tau = \omega_{pe}t_{fin} \simeq 535$). We investigated both the electron and ion behaviour for four different ion masses, $1m_p$, $4m_p$, $16m_p$ and $40m_p$. We investigated the role of the different ion masses because the rate of energy transfer into the ions by electron scattering is different and the period for any ion oscillation will be different. In all of the calculations, $C = 0.02$ and the density was 10^9 cm^{-3}.

Figure 8 shows $1/\Gamma_e$ as a function of time; multiply this result by 2.69 K to get the actual electron temperature. Figure 9 shows the fraction of free electrons as a function of time. For these two parameters, there is not a large effect due to the ion mass. The fraction of free electrons (defined by electrons outside of $0.2a_{ws}$ from any ion) quickly drops to 0.86 by scaled time $\tau \simeq 44$ and then slowly decreases to 0.82 by $\tau \sim 200$. From scaled time 300 to 535, the number of free electron decreases by less than 0.5% when the ion mass is $1m_p$ which means that net recombination almost stops. The net recombination comes from the interplay of the recombination at that time and the electron impact ionization of previously formed atoms. For the heavier ion masses, the number of free electrons slightly increases which indicates that more atoms are being ionized than are forming from recombination. Although the net recombination has essentially stopped or even slightly reversed, the temperature continues to substantially increase over this time range. The scaled temperature Γ_e^{-1} increases from $\simeq 1.7$ at scaled time $\tau = 80$ to $\simeq 2.3$ at $\tau = 300$. From scaled time 300 to 535, the scaled temperature increases to 2.7. The temperature continues to increase even though atom formation almost stops because the electron collisions with the already formed atoms cause the bound electrons to go to deeper binding (lower energy) and thus the

free electrons' kinetic energy must increase. The final scaled temperature of ∼2.7 corresponds to an electron Coulomb coupling of $1/2.7 = 0.37$ if the density were unchanged. Since the density of free electrons decreases by the factor 0.82, the actual electron Coulomb coupling parameter is slightly decreased to $0.82^{1/3}/2.7 = 0.35$.

Figure 10 shows the ion temperature as a function of time (this is the same time range as in figures 8 and 9). Here, there is a clear difference between the calculations with the different ion mass. The smaller ion masses clearly show the effect of electron scattering because there is a rising temperature at the later times. The early time slope of the temperature is proportional to $m_i^{-1/2}$. There are few oscillations of the ion temperature for the $1m_p$ case because the electron temperature is low which leads to a small Debye length.

6. Conclusions

We have investigated some of the early time properties of ultracold neutral plasmas. We have found that the time development of the electron temperature when starting with electrons launched from near the ions is similar to that in a previous study [7] after a time $\sim 1/\omega_{pe}$. If the electrons are launched at zero energy relative to the vacuum threshold, the temperature will increase to give $\Gamma_e \simeq 0.56$ after only ∼11 electron plasma periods; this Γ_e is somewhat lower than in [7] because electron–ion scattering transferred energy from the electrons to the ions in their calculation because of the small ion mass ($m_i = 100m_e$) they used. We found that the early time electron temperature depends on the ion mass because electron scattering can transfer energy from the electrons to the ions.

We investigated how the ion temperature (defined to be 2/3 of the average kinetic energy) evolved as a function of time. We found that we could get good agreement between a full calculation of the ion–electron motion and a calculation using the Debye screening plus a Langevin heating if the electron temperature was larger than ∼25 K corresponding to $\Gamma_e \simeq 0.11$. We found increasing disagreement as the Coulomb coupling parameter changed from $\Gamma_e \simeq 0.23$ to $\Gamma_e \simeq 0.35$. Our results are suggestive, not definitive, that the electron–ion thermalization rate is not accurate at low temperature. There is a proposal to laser cool ions to reach the strongly coupled regime [24] which will be affected by the ion–electron scattering rate; thus, a more detailed study of this issue seems to be warranted.

Finally, we showed results when the electrons are launched at threshold for times out to 300 ns. We found that the mass of the ion did not have a strong effect on the electron properties of the plasma but did have an effect on the ion motion in ways that would be expected from simple arguments. We found that approximately 17% of the ions captured electrons to become Rydberg atoms and that there was no need to invoke exotic effects for this system because the electrons almost immediately evolve out of the strongly coupled regime and become more weakly coupled with time.

Acknowledgments

We thank S Bergeson for discussions related to this system. This work was supported by the Chemical Sciences, Geosciences, and Biosciences Division of the Office of Basic Energy Sciences, US Department of Energy.

References

[1] Killian T, Pattard T, Pohl T and Rost J 2007 *Phys. Rep.* **449** 77
[2] Kulin S, Killian T C, Bergeson S D and Rolston S L 2000 *Phys. Rev. Lett.* **85** 318
[3] Killian T C, Lim M J, Kulin S, Dumke R, Bergeson S D and Rolston S L 2001 *Phys. Rev. Lett.* **86** 3759
[4] Mazevet S, Collins L A and Kress J D 2002 *Phys. Rev. Lett.* **88** 055001
[5] Robicheaux F and Hanson J D 2002 *Phys. Rev. Lett.* **88** 055002
[6] Kuzmin S G and O'Neil T M 2002 *Phys. Rev. Lett.* **88** 065003
[7] Kuzmin S G and O'Neil T M 2002 *Phys. Plasmas* **9** 3743
[8] Robicheaux F and Hanson J D 2003 *Phys. Plasmas* **10** 2217
[9] Pohl T, Pattard T and Rost J M 2004 *Phys. Rev.* A **70** 033416
[10] Simien C E, Chen Y C, Gupta P, Laha S, Martinez Y N, Mickelson P G, Nagel S B and Killian T C 2004 *Phys. Rev. Lett.* **92** 143001
[11] Chen Y C, Simien C E, Laha S, Gupta P, Martinez Y N, Mickelson P G, Nagel S B and Killian T C 2004 *Phys. Rev. Lett.* **93** 265003
[12] Murillo M S 2006 *Phys. Rev. Lett.* **96** 165001
[13] Denning A, Bergeson S D and Robicheaux F 2009 *Phys. Rev.* A **80** 033415
[14] Bergeson S D, Denning A, Lyon M and Robicheaux F 2011 *Phys. Rev.* A **83** 023409
[15] Morrison J P, Rennick C J, Keller J S and Grant E R 2008 *Phys. Rev. Lett.* **101** 205005
[16] Morrison J P, Rennick C J and Grant E R 2009 *Phys. Rev.* A **79** 062706
[17] Saquet N, Morrison J P, Schulz-Weiling M, Sadeghi H, Yiu J, Rennick C J and Grant E R 2011 *J. Phys. B: At. Mol. Opt. Phys.* at press
[18] Press W H, Teukolsky S A, Vetterling W T and Flannery B P 1992 *Numerical Recipes* 2nd edn (New York: Cambridge University Press)
[19] Murillo M S 2007 *Phys. Plasmas* **14** 055702
[20] Daligut J and Dimonte G 2008 *Phys. Rev. Lett.* **101** 135001
[21] Glosli J N, Graziani F R, More R M, Murillo M S, Streitz F H, Surh M P, Benedict L X, Hau-Riege S, Langdon A B and London R A 2008 *Phys. Rev.* E **78** 025401
[22] Gericke D O, Murillo M S and Schlanges M 2002 *Phys. Rev.* E **65** 036418
[23] Pohl T, Pattard T and Rost J M 2005 *J. Phys. B: At. Mol. Opt. Phys.* **38** S343
[24] Pohl T, Pattard T and Rost J M 2004 *Phys. Rev. Lett.* **92** 155003
[25] Pohl T, Pattard T and Rost J M 2005 *Phys. Rev. Lett.* **94** 205003